J Therm Anal Calorim (2014) 115:841–852
DOI 10.1007/s10973-013-3210-4

Theoretical studies of electronic structure and structural properties of anhydrous alkali metal oxalates

Part II. Electronic structure and bonding properties versus thermal decomposition pathway

A. Koleżyński · A. Małecki

Received: 8 January 2013 / Accepted: 19 April 2013 / Published online: 16 May 2013

Abstract The theoretical analysis of electronic structure and bonding properties of anhydrous alkali metal oxalates, based on the results of DFT FP-LAPW calculations, Bader's QTAIM topological properties of electron density, Cioslowski and Mixon's topological bond orders [reported in the first part of this paper by Koleżyński (doi: 10.1007/s10973-013-3126-z)] and Brown's Bond Valence Model calculations, carried out in the light of thermal decomposition pathway characteristic for these compounds are presented. The obtained results shed some additional light on the origins of the complex pathway observed during thermal decomposition process (two stage process, first the formation of respective carbonate and then decomposition to metal oxide and carbon dioxide). For all structures analyzed, strong similarities in electronic structure and bonding properties were found (ionic-covalent bonds in oxalate anion with C–C bond as the weakest one in entire structure and almost purely ionic between oxalate group and alkali metal cations), allowing us to propose the most probable pathway consisting of consecutive steps, leading to carbonate anion formation with simultaneous cationic sublattice relaxations, which results in relative ease of respective metal carbonate formation.

Keywords FP-LAPW ab initio calculations · Electron density topology · Bond order · Bond valence · Thermal decomposition

A. Koleżyński (✉) · A. Małecki
Faculty of Materials Science and Ceramics, AGH University of Science and Technology, Al. Mickiewicza 30, 30-059 Kraków, Poland
e-mail: andrzej.kolezynski@agh.edu.pl

Introduction

Anhydrous alkali metal oxalates $M_2C_2O_4$ form an interesting group of compounds with very similar layered crystal structures and well-defined oxalate anions as an independent entity surrounded by metallic cation and decompose thermally via two step process with respective carbonate as an intermediate product [2–11]:

$$M_2C_2O_4 \rightarrow MCO_3 + CO \rightarrow MO + CO + CO_2$$

which differ significantly from the thermal decomposition pathway characteristic for anhydrous transition metal oxalates (one-step process following either $M_2C_2O_4 \rightarrow MO + CO + CO_2$ or $M_2C_2O_4 \rightarrow M + 2CO_2$ pathway).

There is still lack of consistent theoretical description and explanation of the pathways of thermal decomposition of anhydrous metal oxalate, despite many experimental results available, but it seems plausible that the electronic structure and chemical bonding properties decide which pathway during thermal decomposition process given compound will follow and thus theoretical studies of these properties should provide us with some important information about the relations between electronic and crystal structure and bonding properties and a pathway of thermal decomposition process and in principle allow us to predict (or at least explain) the pathway experimentally observed for given compound. Our theoretical approach based on the topological analysis of electron density (Bader's Quantum Theory of Atoms in Molecules [12] formalism) obtained from first principles FP-LAPW calculations and structural and bonding properties—bonds valence, bond strength, and stresses associated with deviation of given structure from ideal one (Brown's Bond Valence Method [13]) applied mostly for transition metal oxalates and presented recently in a series of papers [14–20] turned out to be very

promising and not only gave us additional insight into the thermal decomposition process in those oxalates but also helped us to describe it as a series of consecutive bond breaking steps proceeding in theoretically predicted order.

The results of similar analysis, carried out for anhydrous alkali metal oxalates are presented in this paper, which due to the size is divided into two parts: first one was devoted to electronic structure and electron density topology analysis and this one deals with bonding properties and thermal decomposition process analyzed in the light of entirety of the obtained results.

Results

The use of empirical correlations between the bond length and strength (valence) of chemical bonds, have a long history in crystal chemistry, starting from Pauling [21]. The present state of the art and perspectives of Bond Valence Model in inorganic crystal chemistry has been reviewed by Urusov and Orlov [22] and recently more extensively by Brown [13].

The "experimental" values of valences s_{ij}^{exp} can be easily calculated from the XRD data and since the sum of such valences will not, in general, be exactly equal to the atomic valence V_i (i.e., will not fulfill the valence sum rule), the measure of the difference between the $\sum s_{ij}^{exp}$ and the expected value V_i, defined as

$$d_i = V_i - \sum_j s'_{ij}$$

can be used for calculating the reliability factor of the crystal structure. A convenient measure of the agreement over the whole structure is given by the index, D, which is the root-mean-square average of the d_i values

$$D = \sqrt{\langle d_i^2 \rangle}$$

Larger values of d_i and D indicate the existence of strained bonds, which can lead to instabilities in the crystal and show most strained regions in the structure (which can simultaneously be the sites of the highest reactivity or liability).

The difference between the theoretically predicted and experimentally observed bond lengths can be used as another indicator of bond strain. In this case, the strain factor δ for a certain group of bonds or the structure as a whole, can be described by following formula:

$$\delta = \sqrt{\frac{\sum_{i=1}^{N} \left(s_i^{theor} - s_i^{exp}\right)^2}{N}}$$

While d_i indicates the magnitude of unbalanced charge for given atom in the structure, the strain factors δ provide us with an additional information about the differences in strains acting on single bonds or group of bonds.

Brown and Shannon [23] pointed out, that bond valence not only measures the number of electrons associated with a bond, but also, in practice, the degree of covalency. Thus, Bond Valence Model can serve as additional (complementary to topological properties of bond critical point and bond order) tool for crystal bond properties analysis. For all structures studied in this paper, as a starting point in BVM analysis, the respective sets of equations (Table 1) consistent with topological properties of electron density (assumed one to one correspondence between bonds and BCPs) has been formulated and solved (assuming C–C bond valence equal to 1). Since the crystal structures of potassium and rubidium (β phase) and cesium and rubidium (α phase) anhydrous oxalates are identical, only the

Table 1 Sets of Valence Sum Rule equations defined within Bond Valence Method formalism for structural and bonding properties analysis of anhydrous alkali metal oxalates

$Li_2C_2O_4$	
$Li = r_1 + r_2 + r_3 + r_4 = {}^1/_4 + {}^1/_4 + {}^1/_4 + {}^1/_4 = 1$	$O_1 = r_2 + r_4 + r_6 = {}^1/_4 + {}^1/_4 + 1^1/_2 = 2$
$C = r_5 + r_6 + r_7 = 1^1/_2 + 1^1/_2 + 1 = 4$	$O_2 = r_1 + r_3 + r_5 = {}^1/_4 + {}^1/_4 + 1^1/_2 = 2$
$Na_2C_2O_4$	
$Na = r_1 + r_2 + r_3 + r_4 = {}^1/_4 + {}^1/_4 + {}^1/_4 + {}^1/_4 = 1$	$O_1 = r_2 + r_3 + r_6 = {}^1/_4 + {}^1/_4 + 1^1/_2 = 2$
$C = r_5 + r_6 + r_7 = 1^1/_2 + 1^1/_2 + 1 = 4$	$O_2 = r_1 + r_4 + r_5 = {}^1/_4 + {}^1/_4 + 1^1/_2 = 2$
$K_2C_2O_4$/β-$Rb_2C_2O_4$	
$K = r_1 + r_2 + r_3 + r_4 = {}^1/_4 + {}^1/_4 + {}^1/_4 + {}^1/_4 = 1$	$O_1 = r_3 + r_4 + r_6 = {}^1/_4 + {}^1/_4 + 1^1/_2 = 2$
$C = r_5 + r_6 + r_7 = 1^1/_2 + 1^1/_2 + 1 = 4$	$O_2 = r_1 + r_2 + r_5 = {}^1/_4 + {}^1/_4 + 1^1/_2 = 2$
$Cs_2C_2O_4$/α-$Rb_2C_2O_4$	
$Cs_1 = r_2 + r_3 + r_4 + r_5 = = {}^1/_4 + {}^1/_4 + {}^1/_4 + {}^1/_4 = 1$	$O_1 = r_2 + r_7 + r_{10} = {}^1/_4 + {}^1/_4 + 1^1/_2 = 2$
$Cs_2 = r_1 + r_6 + r_7 + r_8 + r_9 = {}^1/_4 + {}^1/_8 + {}^1/_4 + {}^1/_8 + {}^1/_4 = 1$	$O_2 = r_5 + r_9 + r_{11} = {}^1/_4 + {}^1/_4 + 1^1/_2 = 2$
$C_1 = r_{10} + r_{11} + r_{14} = 1^1/_2 + 1^1/_2 + 1 = 4$	$O_3 = r_1 + r_{13} = {}^1/_4 + 1^3/_4 = 2$
$C_2 = r_{12} + r_{13} + r_{14} = 1^1/_4 + 1^3/_4 + 1 = 4$	$O_4 = r_3 + r_4 + r_6 + r_8 + r_{12} = {}^1/_4 + {}^1/_4 + {}^1/_8 + {}^1/_8 + 1^1/_4 = 2$

equations for potassium and cesium oxalates are presented here. The results of BVM calculations carried out for anhydrous alkali metal oxalates are presented in Tables 2, 4, 6, 8, 10 and 12 (calculated bond valences with residual strain factors d_i and D) and Tables 3, 5, 7, 9, 11 and 13 (theoretical bond valences and bond lengths calculated according to valence sum rule equations and bonds strain factors δ for bond groups and the whole structure).

Anhydrous lithium oxalate

Data presented in Table 2 show that the crystal structure of anhydrous lithium oxalate is characterized by very small degree of deviation from ideal one (global instability index D equal to 0.11 valence units) and in the proximity of every atom in this structure all bonds are too long on average—evidently this is the results of necessary compromise between bond lengths inside oxalate anion constraining possible system geometry and minimization of electrostatic interactions between lithium cations and oxalate anions. The environments of carbon and oxygen O_1 atoms are most deviated ones in the structure ($d_i \cong 0.14$ v.u.), while in case of lithium atoms this deviation is much smaller ($d_i \cong 0.07$ v.u.) and for oxygen O_2 it is practically negligible (d_i below 0.03 v.u.).

The results presented in Table 3 complement the above analysis: three Li–O bonds (r_2–r_4) are too long and one (r_1) is too short. Oxygen atom O_1 forms three bonds: two of them—with carbon and lithium, (r_4 and r_6, respectively)—much too long and most strongly stretched and the third (r_2) close to ideal one. This results in average length of the bonds created by O_1 atom significantly longer than in ideal structure. Similarly, all bonds formed by carbon atom are too long leading to the highest deviation of its environment in comparison to ideal structure. O_2 atom forms two bonds with lithium (r_1 is too short and r_3 too long, similarly deviated from ideal ones), and one slightly too long, with carbon (r_5), which results in almost total stress cancellation.

Presented results, together with electronic structure and topological properties presented in Part I of this paper [1] show that in anhydrous lithium oxalate structure C–C bond is the weakest one and one can safely assume that during thermal decomposition process this bond should break as a first one. Since the strains in this structure are relatively small, one can expect their moderate relaxation and charge transfer to remaining bonds regions. The prediction of the next step in this structure is difficult, since naïve analysis based on bond orders would suggest wrongly thermal decomposition to metal and carbon dioxide (similar to e.g., anhydrous cadmium or silver oxalate [14, 15]). But it is well-known from the experiment [24, 25] that anhydrous lithium oxalate decompose thermally to lithium carbonate and then—in much higher temperature—to lithium oxide. What is more, such process of formation of metallic lithium would necessitate quite big charge transfer from oxygen atoms in COO^- anions to lithium cations, which

Table 2 The results of BVM analysis carried out for anhydrous lithium oxalate: bond and atomic valences s_{ij} and V_{ij}, atomic residual strain factors d_i and global structure instability index D

$Li_2C_2O_4$						V_{ij}	d_i	D
Li		O_2	O_1	O_2	O_1	0.927	0.073	0.107
	R_{ij}	1.935	1.999	2.033	2.076			
	s_{ij}	0.282	0.237	0.216	0.192			
O_1		Li	Li	C		1.863	0.137	
	R_{ij}	1.999	2.076	1.257				
	s_{ij}	0.237	0.192	1.434				
O_2		Li	Li	C		1.971	0.029	
	R_{ij}	1.935	2.033	1.247				
	s_{ij}	0.282	0.216	1.473				
C		O_2	O_1	C		3.856	0.144	
	R_{ij}	1.247	1.257	1.559				
	s_{ij}	1.473	1.434	0.949				

Table 3 The results of BVM analysis carried out for anhydrous lithium oxalate: bond valences s_{ij}^{calc} calculated for experimental bond lengths R_{exp}, theoretical bond valences calculated from Valence Sum Rule equations s_{ij}^{theor}, experimental and theoretical bond lengths R_{exp} and R_{theor}, relative bond differences $\Delta R/R$ and bond strain factors δ

$Li_2C_2O_4$	s_{ij}^{calc}	s_{ij}^{theor}	R_{exp}/Å	R_{theor}/Å	$\Delta R/R$/%	δ			
r_1 (Li–O_2)	0.282	¼	1.935	1.979	−2.28	δ_{Li-O}	0.038	δ_{Li-O2a}	0.032
r_2 (Li–O_1)	0.237	¼	1.999	1.979	0.99			δ_{Li-O1a}	0.013
r_3 (Li–O_2)	0.216	¼	2.033	1.979	2.65			δ_{Li-O2b}	0.034
r_4 (Li–O_1)	0.192	¼	2.076	1.979	4.69			δ_{Li-O1b}	0.058
r_5 (C–O_2)	1.473	1½	1.247	1.240	0.54	δ_{C-O}	0.050	δ_{C-O2}	0.027
r_6 (C–O_1)	1.434	1½	1.257	1.240	1.32			δ_{C-O1}	0.066
r_7 (C–C)	0.949	1	1.559	1.540	1.24	δ_{C-C}	0.051		
						δ_{Struct}	0.044		

taking into account their calculated net charge equal to +0.85e and the difference in electronegativity between oxygen and lithium and strongly ionic character of Li–O bonds is not plausible and one can safely assume that much more probable is the process of breaking of these bonds, without charge transfer between lithium and oxygen and setting COO^- anions free inside the gaps within cationic sub-lattice.

Therefore, in our opinion, the pathway of thermal decomposition of anhydrous lithium oxalate is as follow: first C–C bond breaks, which leads to freeing of COO^- anions (connected with cationic sub-lattice via non-directional ionic bonds) and to breaking of these ionic bonds in the next step, which allow these anions to change the position and spatial orientation within coordination polyhedron built from twelve lithium cations quite easily and leads to the formation of intermediate $[OCOCO_2]^{2-}$ anions, which afterward decompose to CO_3^{2-} anions and carbon oxide(II) molecules, according to the following reaction [4, 26]:

$$C_2O_4^{2-} \Leftrightarrow 2COO^- \rightarrow [OCOCO_2]^{2-} \rightarrow CO_3^{2-} + CO$$

The final step in thermal decomposition process consists of the structural alteration, which—due to very high similarity of anhydrous lithium oxalate and lithium carbonate structures [27]—is relatively small (Fig. 1) and leads to lithium carbonate as a final product, in agreement with the experimental findings [24, 25].

Table 4 The results of BVM analysis carried out for anhydrous sodium oxalate: bond and atomic valences s_{ij} and V_{ij}, atomic residual strain factors d_i and global structure instability index D

$Na_2C_2O_4$						V_{ij}	d_i	D
Na		O_2	O_1	O_1	O_2	0.907	0.093	0.148
	R_{ij}	2.320	2.331	2.343	2.422			
	s_{ij}	0.247	0.234	0.232	0.188			
O_1		Na	Na	C		1.875	0.125	
	R_{ij}	2.331	2.343	1.265				
	s_{ij}	0.234	0.232	1.403				
O_2		Na	Na	C		1.881	0.119	
	R_{ij}	2.320	2.422	1.253				
	s_{ij}	0.247	0.188	1.447				
C		O_2	O_1	C		3.778	0.222	
	R_{ij}	1.253	1.265	1.567				
	s_{ij}	1.447	1.403	0.929				

Anhydrous sodium oxalate

Similar analysis can be carried out for the rest of the structures and thus, due to some space limitations, we will focus in the rest of our paper on most important results only and present a concise analysis done on their basis. The results presented in Table 4 show that the crystal structure of anhydrous sodium oxalate is only slightly deviated from ideal one ($D \cong 0.15$ v.u.) and for all atoms the bonds they are creating are too long, a compromise between bonds lengths within oxalate anion and Na–O bonds—similarly as in lithium oxalate. The environments of carbon atoms are most strongly deviated ($d_i \cong 0.22$ v.u.) while for the other atoms such deviation is significantly smaller ($d_i \cong 0.1$–0.13 v.u.).

The data presented in Table 5 shed some additional light on the structural properties of sodium oxalate: all Na–O bonds (r_1–r_4) are too long and r_4 is most strongly stretched. O_1 atom forms three too long bonds: Na–O (r_2, r_3) and C–O (r_6) and this last one is most strongly strained one in the entire structure ($\delta_{C-O1} = 0.1$). Among three bonds formed by O_2 atoms (r_1, r_4, and r_5) most strongly stretched is the longest one Na–O_2 (r_4) and slightly weaker C–O_2 (r_5) while the second Na–O_2 bond (r_1) is practically relaxed. Carbon atom forms three, strongly strained bonds ($\delta \cong 0.05$, 0.1 and 0.07, for r_5, r_6, and r_7 respectively).

Since the results of calculations of electronic structure and topological properties of electron density and BVM analysis carried out for anhydrous sodium oxalate are very similar to these obtained for lithium oxalate, one can

Table 5 The results of BVM analysis carried out for anhydrous sodium oxalate: "experimental" s_{ij}^{calc} and theoretical s_{ij}^{theor} bond valences, experimental and theoretical bond lengths R_{exp} and R_{theor}, relative bond differences $\Delta R/R$ and bond strain factors δ

$Na_2C_2O_4$	s_{ij}^{calc}	s_{ij}^{theor}	R_{exp}/Å	R_{theor}/Å	$\Delta R/R$/%	δ			
r_1 (Na–O_2)	0.247	¼	2.320	2.316	0.18	δ_{Na-O}	0.033	δ_{Na-O2a}	0.003
r_2 (Na–O_1)	0.240	¼	2.331	2.316	0.65			δ_{Na-O1a}	0.010
r_3 (Na–O_1)	0.232	¼	2.343	2.316	1.16			δ_{Na-O1b}	0.018
r_4 (Na–O_2)	0.188	¼	2.422	2.316	4.39			δ_{Na-O2b}	0.062
r_5 (C–O_2)	1.447	1½	1.253	1.240	1.07	δ_{C-O}	0.079	δ_{C-O2}	0.053
r_6 (C–O_1)	1.402	1½	1.265	1.240	1.97			δ_{C-O1}	0.098
r_7 (C–C)	0.929	1	1.567	1.540	1.74	δ_{C-C}	0.071		
						δ_{Struct}	0.056		

expect to find analogous to the described above series of consecutive steps of bonds breaking/forming during thermal decomposition process and decomposition of anhydrous sodium oxalate to sodium carbonate [28, 29] (since both oxalate and carbonate structures are very similar—such structural alteration can go very easily [30] (Fig. 2).

$K_2C_2O_4$

From Table 6 follows that the crystal structure of anhydrous potassium oxalate deviates quite strongly from the ideal one ($D \cong 0.29$) and all bonds are too long on average (again as a result of a compromise between lengths of relatively rigid mostly covalent bonds inside oxalate anions and lengths of ionic K–O bonds and repulsion forces between potassium cations). In this case most deviated ones are potassium atoms environments ($d_i \cong 0.42$ v.u.)—despite as much as eight K–O bonds, since they are significantly too long and their valences too small to fully compensate potassium cation formal valence (+1). For the rest of atoms these deviations are much smaller, but still significant ($d_i \cong 0.2$–0.26 v.u.).

Data presented in Table 7 confirm the above conclusions: all bonds in the structure are subjected to tension and C–C bonds are most strongly stretched. K–O bonds (r_1–r_4) are definitely too long (with strains similar to those acting on C–C bonds) and potassium atom environment is most deviated from ideal structure. O_1 atom forms two strongly stretched bonds with potassium (r_3, r_4) and one much weaker strained with carbon (r_6). Analogously O_2 creates two shorter and thus slightly less stretched bonds with potassium (r_1, r_2) and much less strained bond with carbon (r_5). Among three bonds created by carbon, the two with oxygen (r_5, r_6) are relatively not much elongated, while C–C bond (r_6) is under strongest strains in the structure.

Presented results show that despite the different crystal structure than in case of lithium and sodium oxalates, the properties of electronic structure, electron density topology and the results of BVM analysis are very similar to those obtained for previous two cases, which allow us to assume the same pathway of thermal decomposition process of anhydrous potassium oxalate as earlier: first C–C bond breaks, which due to excessive thermal energy leads to breaking free of remaining COO^- anions and next, as a result of their translational and rotational movements leads to the formation of unstable $[OCOCO_2]^{2-}$ anions, which afterward decompose to CO_3^{2-} anions and carbon oxide(II) molecules [31–33]. The final step of this process consists of the structural alteration, which—due to very high similarity of anhydrous potassium oxalate and potassium carbonate structures—should undergo very easily, resulting in the formation of potassium carbonate as a final product of thermal decomposition process (topochemical reaction [26]).

Table 6 The results of BVM analysis carried out for anhydrous potassium oxalate: bond and atomic valences s_{ij} and V_{ij}, atomic residual strain factors d_i and global structure instability index D

$K_2C_2O_4$						V_{ij}	d_i	D
K		O_2	O_2	O_1	O_1	0.582	0.418	0.286
	R_{ij}	2.806	2.839	2.842	2.901			
	s_{ij}	0.162	0.148	0.147	0.125			
O_1		K	K	C		1.738	0.262	
	R_{ij}	2.842	2.901	1.249				
	s_{ij}	0.147	0.125	1.466				
O_2		K	K	C		1.786	0.214	
	R_{ij}	2.806	2.839	1.246				
	s_{ij}	0.162	0.148	1.476				
C		O_2	O_1	C		3.804	0.196	
	R_{ij}	1.246	1.249	1.595				
	s_{ij}	1.476	1.466	0.862				

α-$Rb_2C_2O_4$

From data in Table 8 follow that crystal structure of anhydrous rubidium oxalate (α phase) deviates quite much

Table 7 The results of BVM analysis carried out for anhydrous potassium oxalate: "experimental" s_{ij}^{calc} and theoretical s_{ij}^{theor} bond valences, experimental and theoretical bond lengths R_{exp} and R_{theor}, relative bond differences $\Delta R/R$ and bond strain factors δ

$K_2C_2O_4$	s_{ij}^{calc}	s_{ij}^{theor}	R_{exp}/Å	R_{theor}/Å	$\Delta R/R$/%	δ			
r_1 (K–O_2)	0.162	¼	2.806	2.645	5.73	δ_{K-O}	0.105	δ_{K-O2a}	0.088
r_2 (K–O_2)	0.148	¼	2.839	2.645	6.82			δ_{K-O2b}	0.102
r_3 (K–O_1)	0.147	¼	2.842	2.645	6.92			δ_{K-O1a}	0.103
r_4 (K–O_1)	0.125	¼	2.901	2.645	8.84			δ_{K-O1b}	0.125
r_5 (C–O_2)	1.476	1½	1.246	1.240	0.47	δ_{C-O}	0.029	δ_{C-O2}	0.024
r_6 (C–O_1)	1.466	1½	1.248	1.240	0.68			δ_{C-O1}	0.034
r_7 (C–C)	0.862	1	1.595	1.540	3.45	δ_{C-C}	0.138		
						δ_{Struct}	0.097		

Table 8 The results of BVM analysis carried out for anhydrous rubidium oxalate (α phase): bond and atomic valences s_{ij} and V_{ij}, atomic residual strain factors d_i and global structure instability index D

α-$Rb_2C_2O_4$							V_{ij}	d_i	D
Rb_1		O_2	O_4	O_1	O_4		0.650	0.350	0.224
	R_{ij}	2.888	2.907	2.953	3.005				
	s_{ij}	0.185	0.175	0.155	0.135				
Rb_2		O_3	O_1	O_4	O_4	O_2	0.656	0.344	
	R_{ij}	2.816	3.030	3.041	3.042	3.293			
	s_{ij}	0.224	0.126	0.122	0.122	0.062			
O_1		Rb_1	Rb_1	C_1			1.756	0.244	
	R_{ij}	2.953	3.030	1.246					
	s_{ij}	0.155	0.126	1.475					
O_2		Rb_1	Rb_2	C_1			1.985	0.015	
	R_{ij}	2.888	3.293	1.185					
	s_{ij}	0.185	0.062	1.739					
O_3		Rb_2	C_2				1.973	0.027	
	R_{ij}	2.816	1.183						
	s_{ij}	0.224	1.749						
O_4		Rb_1	Rb_1	Rb_2	Rb_2	C_2	2.012	−0.012	
	R_{ij}	2.907	3.005	3.041	3.042	1.250			
	s_{ij}	0.175	0.135	0.122	0.122	1.458			
C_1		O_2	O_1	C_2			4.225	−0.225	
	R_{ij}	1.185	1.246	1.536					
	s_{ij}	1.739	1.475	1.011					
C_2		O_3	O_4	C_1			4.218	−0.218	
	R_{ij}	1.183	1.250	1.536					
	s_{ij}	1.749	1.458	1.011					

Table 9 The results of BVM analysis carried out for anhydrous rubidium oxalate (α phase): "experimental" s_{ij}^{calc} and theoretical s_{ij}^{theor} bond valences, experimental and theoretical bond lengths R_{exp} and R_{theor}, relative bond differences $\Delta R/R$ and bond strain factors δ

α-$Rb_2C_2O_4$	s_{ij}^{calc}	s_{ij}^{theor}	R_{exp}/Å	R_{theor}/Å	$\Delta R/R$/%	δ			
r_1 (Rb_2–O_3)	0.185	¼	2.816	2.776	1.43	δ_{Rb1-O}	0.090	δ_{Rb2-O3}	0.065
r_2 (Rb_1–O_2)	0.175	¼	2.888	2.776	3.87			δ_{Rb1-O2}	0.075
r_3 (Rb_1–O_4)	0.155	¼	2.907	2.776	4.52			δ_{Rb1-O4}	0.095
r_4 (Rb_1–O_1)	0.135	¼	2.953	2.776	5.99			δ_{Rb1-O1}	0.115
r_5 (Rb_1–O_4)	0.224	¼	3.005	2.776	7.62	δ_{Rb2-O}	0.101	δ_{Rb1-O4}	0.026
r_6 (Rb_2–O_1)	0.126	¼	3.030	2.776	8.38			δ_{Rb2-O1}	0.124
r_7 (Rb_2–O_4)	0.122	$^1/_8$	3.040	3.032	0.27			$\delta_{Rb2-O4a}$	0.003
r_8 (Rb_2–O_4)	0.122	$^1/_8$	3.042	3.032	0.32			$\delta_{Rb2-O4b}$	0.003
r_9 (Rb_2–O_2)	0.062	¼	3.293	2.776	15.70			δ_{Rb2-O2}	0.188
r_{10} (C_2–O_3)	1.749	1¾	1.183	1.183	0.02	δ_{C1-O}	0.170	δ_{C2-O3}	0.001
r_{11} (C_1–O_2)	1.738	1½	1.185	1.240	−4.61			δ_{C1-O2}	0.238
r_{12} (C_1–O_1)	1.475	1½	1.246	1.240	0.50	δ_{C2-O}	0.147	δ_{C1-O1}	0.025
r_{13} (C_2–O_4)	1.458	1¼	1.250	1.307	−4.56			δ_{C2-O4}	0.208
r_{14} (C_1–C_2)	1.011	1	1.536	1.540	−0.27	δ_{C-C}	0.011		
						δ_{Struct}	0.115		

from the ideal one ($D \cong 0.22$) and the strongest deviation characterizes the environment of two symmetrically non-equivalent rubidium atoms ($d_i \cong 0.35$ v.u.), which despite different coordination numbers and thus different number of bonds (4 and 5), form bonds which are too long and are subjected to strong tensile strains. Much less deviated are the environments of carbon ($d_i \cong -0.22$ v.u.; on average bonds too short, thus subjected to compressive strains) and O_1 oxygen ($d_i \cong +0.24$ v.u.; bonds on average too long and under tensile strains), while the environments of the remaining oxygen atoms (O_2–O_4) are almost not deviated from ideal ones.

Additional information about the amount of strains acting locally on atoms and thus about decomposition process provide data presented in Table 9. The strongest compressive strains act on two C–O bonds C–O (r_{11} and r_{13}; δ above 0.2), while two remaining C–O bonds (r_{10} and r_{12}) are almost unaltered. Analogously strong strains as on bonds (r_{11} and r_{13}), but tensile this time, act on Rb_2–O_2 bond (r_9, $\delta \cong 0.19$), much weaker on three Rb–O bonds (r_1–r_4 and r_6, $\delta = 0.07$–0.12) and very weak ones on Rb_1–O_4 bond (r_5, $\delta = 0.03$). Rb_2–O_4 and C–C (r_7, r_8, and r_{14}, respectively) are almost relaxed. Rubidium atoms Rb_1 and Rb_2 form respectively four (r_2–r_5) and five (r_1, r_6–r_9) significantly too long bonds, resulting in high deviations of their environments from ideal ones. One can see here easily the results of very difficult-to-reach compromise between bond lengths in rigid structure of oxalate anions with directional ionic-covalent and covalent bonds and optimal length for purely electrostatic non-directional ionic Rb–O bonds. Oxygen O_1 forms two, too long bonds with rubidium (r_4, r_6) and slightly too long with carbon (r_{12}), resulting in high strains in its environment. In case of C_1 and C_2 carbon atoms, high deviation of their environments results from strong asymmetry of strains acting on C–O bonds: one of them is much too short (r_{11} and r_{13}) while the second one (r_{10} and r_{12}) slightly too long, which—with almost relaxed C–C bond –leads to resultant compressive strains acting in the environments of carbon atoms. Two oxygen atoms (O_2 and O_4) form two, too short bonds with rubidium (O_4 creates yet two additional, practically relaxed Rb–O_4) and in the same time one too short bond with carbon, resulting in almost zero resultant deviation of their environments from ideal one. The last oxygen atom O_3 forms one, slightly too long bond with Rb (r_1) and one almost relaxed with carbon (r_{10}) resulting in a very small deviation of its environment ($d_i \cong 0.03$).

The results obtained for anhydrous α-rubidium oxalate (presented in Part I of this paper [1]) show that the features of electronic structure and topological properties of chemical bonds are very similar to those found for all above analyzed alkali metal oxalate. Also valences and strains acting on bonds and atomic environments, calculated according to BVM formalism are qualitatively very similar to the above ones. Therefore one can expect to find similar mechanism of thermal decomposition process with similar pathway in this case as well, leading to identical final results. This supposition is confirmed by experimental

Table 10 The results of BVM analysis carried out for anhydrous rubidium oxalate (β phase): bond and atomic valences s_{ij} and V_{ij}, atomic residual strain factors d_i and global structure instability index D

β-$Rb_2C_2O_4$						V_{ij}	d_i	D
Rb		O_2	O_2	O_1	O_1	0.542	0.458	0.273
	R_{ij}	2.960	2.988	3.018	3.051			
	s_{ij}	0.152	0.141	0.130	0.119			
O_1		Rb	Rb	C		1.767	0.233	
	R_{ij}	3.018	3.051	1.236				
	s_{ij}	0.130	0.119	1.518				
O_2		Rb	Rb	C		2.024	−0.024	
	R_{ij}	2.960	2.988	1.187				
	s_{ij}	0.152	0.141	1.731				
C		O_2	O_1	C		4.180	−0.180	
	R_{ij}	1.187	1.236	1.567				
	s_{ij}	1.731	1.518	0.931				

Table 11 The results of BVM analysis carried out for anhydrous rubidium oxalate (β phase): "experimental" s_{ij}^{calc} and theoretical s_{ij}^{theor} bond valences, experimental and theoretical bond lengths R_{exp} and R_{theor}, relative bond differences $\Delta R/R$ and bond strain factors δ

β-$Rb_2C_2O_4$	s_{ij}^{calc}	s_{ij}^{theor}	R_{exp}/Å	R_{theor}/Å	$\Delta R/R$/%	δ			
r_1 (Rb–O_2)	0.152	¼	2.960	2.776	6.21	δ_{Rb-O}	0.115	δ_{Rb-O2a}	0.098
r_2 (Rb–O_2)	0.141	¼	2.988	2.776	7.10			δ_{Rb-O2b}	0.109
r_3 (Rb–O_1)	0.130	¼	3.018	2.776	8.02			δ_{Rb-O1a}	0.120
r_4 (Rb–O_1)	0.119	¼	3.051	2.776	9.01			δ_{Rb-O1b}	0.131
r_5 (C–O_2)	1.731	1½	1.187	1.240	−4.47	δ_{C-O}	0.164	δ_{C-O2}	0.231
r_6 (C–O_1)	1.518	1½	1.236	1.240	−0.36			δ_{C-O1}	0.018
r_7 (C–C)	0.930	1	1.567	1.540	1.70	δ_{C-C}	0.070		
						δ_{Struct}	0.126		

Table 12 The results of BVM analysis carried out for anhydrous cesium oxalate: bond and atomic valences s_{ij} and V_{ij}, atomic residual strain factors d_i and global structure instability index D

$Cs_2C_2O_4$							V_{ij}	d_i	D
Cs_1		O_1	O_4(a)	O_4(b)	O_2		0.647	0.353	0.339
	R_{ij}	3.069	3.081	3.089	3.129				
	s_{ij}	0.172	0.166	0.163	0.146				
Cs_2		O_3	O_4(a)	O_1	O_4(b)	O_2	0.658	0.342	
	R_{ij}	3.015	3.135	3.181	3.223	3.372			
	s_{ij}	0.199	0.144	0.127	0.113	0.076			
O_1		Cs_1	Cs_2	C_1			1.670	0.330	
	R_{ij}	3.069	3.181	1.273					
	s_{ij}	0.172	0.127	1.371					
O_2		Cs_1	Cs_2	C_1			1.591	0.409	
	R_{ij}	3.129	3.372	1.274					
	s_{ij}	0.146	0.076	1.369					
O_3		Cs_2	C_2				1.562	0.438	
	R_{ij}	3.015	1.275						
	s_{ij}	0.199	1.363						
O_4		Cs_1(a)	Cs_1(b)	Cs_2(a)	Cs_2(b)	C_2	1.950	0.050	
	R_{ij}	3.081	3.089	3.135	3.223	1.275			
	s_{ij}	0.166	0.163	0.144	0.113	1.364			
C_1		O_1	O_2	C_2			3.686	0.314	
	R_{ij}	1.273	1.274	1.560					
	s_{ij}	1.371	1.369	0.946					
C_2		O_4	O_3	C_1			3.674	0.326	
	R_{ij}	1.275	1.275	1.560					
	s_{ij}	1.364	1.363	0.946					

Table 13 The results of BVM analysis carried out for anhydrous cesium oxalate: "experimental" s_{ij}^{calc} and theoretical s_{ij}^{theor} bond valences, experimental and theoretical bond lengths R_{exp} and R_{theor}, relative bond differences $\Delta R/R$ and bond strain factors δ

$Cs_2C_2O_4$	s_{ij}^{calc}	s_{ij}^{theor}	R_{exp}/Å	R_{theor}/Å	$\Delta R/R$/%	δ			
r_1 (Cs_2–O_3)	0.199	¼	3.015	2.930	2.83	δ_{Cs1-O}	0.089	δ_{Cs2-O3}	0.051
r_2 (Cs_1–O_1)	0.172	¼	3.069	2.930	4.52			δ_{Cs1-O1}	0.078
r_3 (Cs_1–O_4)	0.166	¼	3.081	2.930	4.90			$\delta_{Cs1-O4a}$	0.084
r_4 (Cs_1–O_4)	0.163	¼	3.089	2.930	5.14			$\delta_{Cs1-O4b}$	0.087
r_5 (Cs_1–O_2)	0.146	¼	3.129	2.930	6.36	δ_{Cs2-O}	0.099	δ_{Cs1-O2}	0.104
r_6 (Cs_2–O_4)	0.144	$^1/_8$	3.135	3.186	−1.65			$\delta_{Cs2-O4a}$	0.019
r_7 (Cs_2–O_1)	0.127	¼	3.181	2.930	7.88			δ_{Cs2-O1}	0.123
r_8 (Cs_2–O_4)	0.113	$^1/_8$	3.223	3.186	1.14			$\delta_{Cs2-O4b}$	0.012
r_9 (Cs_2–O_2)	0.076	¼	3.372	2.930	13.10			δ_{Cs2-O2}	0.174
r_{10} (C_1–O_1)	1.371	1½	1.273	1.240	2.61	δ_{C1-O}	0.130	δ_{C1-O1}	0.129
r_{11} (C_1–O_2)	1.369	1½	1.274	1.240	2.65			δ_{C1-O2}	0.131
r_{12} (C_2–O_4)	1.364	1¼	1.275	1.307	−2.54	δ_{C2-O}	0.285	δ_{C2-O4}	0.114
r_{13} (C_2–O_3)	1.363	1¾	1.275	1.183	7.25			δ_{C2-O3}	0.387
r_{14} (C_1–C_2)	0.946	1	1.560	1.540	1.31	δ_{C-C}	0.054		
						δ_{Struct}	0.141		

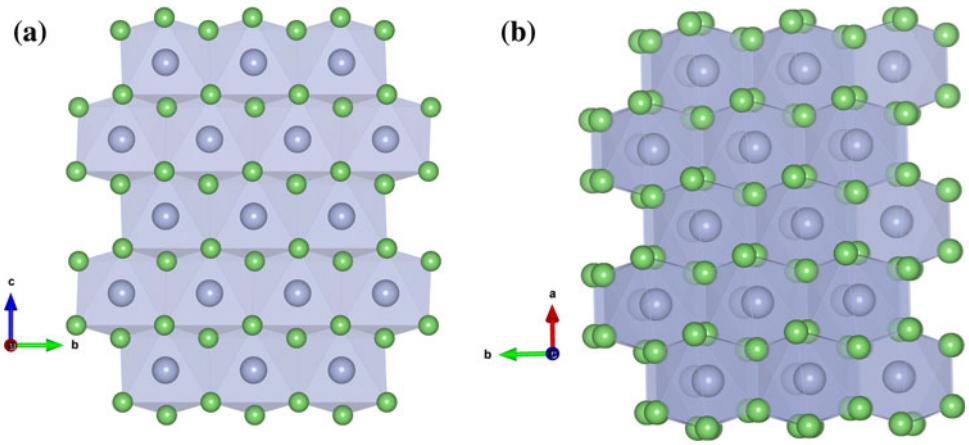

Fig. 1 Comparison of anhydrous lithium oxalate (**a**) and lithium carbonate (**b**) crystal structure. To emphasize structure similarities, $C_2O_4^{2-}$ and CO_3^{2-} anions have been replaced by *balls* (*bigger* and *lighter*), placed in the centers of mass of respective anions

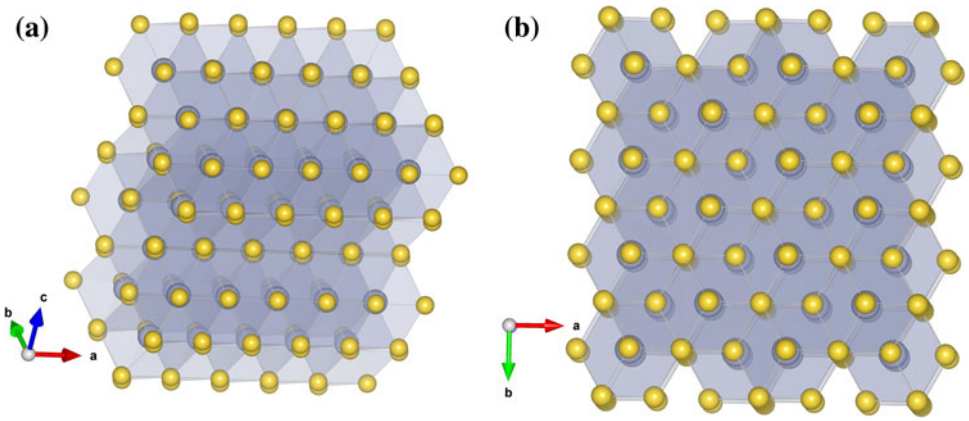

Fig. 2 Anhydrous sodium oxalate (**a**) and sodium carbonate (**b**) crystal structures. To emphasize the similarities of these structures, $C_2O_4^{2-}$ and CO_3^{2-} anions have been replaced by *balls* placed in the centers of mass of respective anions (*bigger ones*)

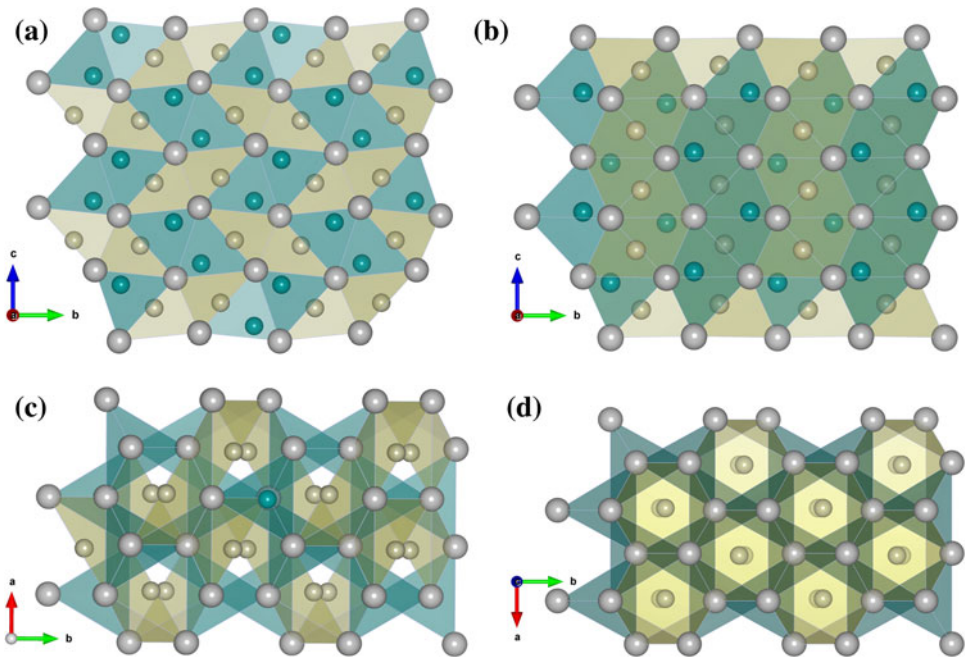

Fig. 3 The comparison of the crystal structures of anhydrous rubidium oxalate (α phase; *left column*) and rubidium carbonate (α phase; *right column*). To emphasize the similarities of both structures, $C_2O_4^{2-}$ and CO_3^{2-} anions have been replaced by *balls* (*bigger ones* in the figure) placed in the center of mass of respective anions

findings—α-$Rb_2C_2O_4$ decomposes thermally to rubidium carbonate and carbon oxide(II) [31, 34, 35].

Detailed analysis of the obtained results allows us to propose the following pathway of thermal decomposition process of anhydrous α-rubidium oxalate: first C–C bond—the weakest one in the structure—breaks, which is followed by breaking free of remaining COO^- anions (breaking Rb–O bonds) and then due to their thermally activated translational and rotational movements leads to the formation of unstable $[OCOCO_2]^{2-}$ anions, subsequently decomposed to CO_3^{2-} anions and carbon oxide(II) molecules. The final step of this process consists of the structure alteration due to the strains relaxation and minimization of the interactions of carbonate anions with cationic sublattice resulting in α-rubidium carbonate crystal structure formation, which due to high similarity of oxalate and carbonate structures (see Fig. 3) should undergo very easily.

β-$Rb_2C_2O_4$

Since the crystal structures of anhydrous β-rubidium and potassium oxalates are very similar to each other (isostructural compounds), one can expect that despite minor differences in electronic structure and bonding properties and strain distribution, in both cases the thermal decomposition process will follow identical pathway. The detailed analysis of the results of electronic structure, electron density topology, and BVM analysis carried out for anhydrous β-rubidium oxalate confirm strongly this supposition (due to some space limitations we have omitted the details of this analysis here and let interested readers to do it by themselves) and allow us to state that also in this case the final products of thermal decomposition process are respective carbonate (β-rubidium carbonate) and carbon oxide(II).

$Cs_2C_2O_4$

Analogously to the last example, the crystal structure of anhydrous cesium oxalate is isostructural with α-rubidium oxalate structure and the results obtained for the former are very similar to the ones obtained for the latter. Thus again, due to the lack of space we have omitted the details of this analysis here and let interested readers to do it by themselves.

The conclusions one can draw from the mentioned analysis are as follow: first C–C bonds break and this is followed by Rb–O bonds breaking and freeing COO^- anions, which due to spatial reorientation and position changing, form a bond between oxygen atom from one anion and carbon atom from the other one, creating unstable intermediate $[OCOCO_2]^{2-}$ anions, decomposed afterward to carbonate anions CO_3^{2-} and carbon oxide(II) molecules. The whole process is ended by structure alteration to minimize the interactions between carbonate anion and cationic sublattice (process energetically not very demanding, since both oxalate and carbonate structures are very similar, therefore it should undergo very easily), resulting in a formation of potassium carbonate as a final product of thermal decomposition process.

Conclusions

Theoretical analysis of the results of FP-LAPW ab initio calculations of electronic structure, total electron density topology (within Bader's QTAIM formalism), and bond valence (Brown's BVM approach) carried out for anhydrous alkali metal oxalates presented in this paper allows us to formulate the following conclusions. The proposed-by-us approach to the problem of thermal decomposition process in oxalates, namely using theoretical methods for the analysis of electronic structure and bonding properties to be able to predict (or at least to explain) the most probable pathway of thermal decomposition process in given oxalate, has been very useful when applied for transition metal anhydrous oxalates [14–20], but in case of alkali metal oxalates has faced some difficulties. These difficulties follow mostly the constraints of the methods used in our approach, which despite the complex treatment of the problem of bonding properties in crystal structure (global: from a point of view of band structure and densities of states, total and projected onto particular atoms and atomic orbitals and local: from a point of view of topological properties of bond critical points and local strains acting on particular bonds) allow analyzing properties permitting to propose the most probable sequence of structure decomposition (bonds breaking and related relaxation and structure alteration processes), but does not allow in a simple way taking into account the bond formation processes, which takes place during thermal decomposition of anhydrous alkali metal oxalates. Therefore this approach, when applied without due consideration, suggests the thermal decomposition to metal and carbon dioxide, in contradiction with the experimentally observed decomposition to metal carbonate and carbon oxide(II). Only more thorough analysis, taking into account not only topological properties of bonds and strains acting on them but also the properties of particular atoms in given structure (especially cations) and their influence on the character and properties of bonds (particularly metal–oxygen bonds, which in our opinion play a key role in thermal decomposition process, determining the decomposition pathway to carbonate, metal or metal oxide) allow explaining dissimilarity of decomposition pathway in case of ionic anhydrous oxalates.

While the topological analysis alone does not show so distinctly the differences of the properties of metal–oxygen bonds between d-electron metal and alkali metal anhydrous oxalates, the results of electronic structure calculations allow distinguishing of such properties very easily, since they show clearly not only how big are the differences resulting from different occupations of electronic shells in particular cations, but also how similar are the partial densities of states distribution projected onto particular atomic orbitals of carbon and oxygen, confirming the conclusions following from structural analysis about comparatively weak influence of the oxalate anion environment (cation type) on the behavior and properties of carbon and oxygen electrons, filling in qualitatively very similar way the same bands with like energies in different oxalate. It is, however, necessary to underline that as it follows from standard quantum mechanical simulation, the isolated oxalate anion tend to assume energetically most stable conformation in which COO^- groups in oxalate anion are rotated against each other by 90° (symmetry D_{2d}), while in most oxalates these anions have planar symmetry (D_{2h}) with only two exceptions known to us (isostructural anhydrous α-rubidium and cesium oxalates), which shows that one cannot completely exclude the interactions between oxalate anions and cationic sub-lattice from theoretical analysis.

The topological analysis of electron density and properties of bond critical points shows that in all analyzed alkali metal anhydrous oxalates C–C bonds are the weakest ones, metal–oxygen bonds are slightly stronger, and carbon–oxygen bonds are the strongest (but the latter differ from the remaining ones in much smaller degree than in case of transition metal oxalates [14–20]). This allows us to formulate a thesis, that in every case of alkali metal oxalate, carbon–carbon bond will break as the first one during thermal decomposition process, resulting in partial structure alteration and strain relaxation. The most probable next step is breaking of Me–O bonds and setting free COO^- anions inside the gaps within cationic sub-lattice, which can either give an electron to nearest cation (highly improbable thermodynamically) or due to thermally activated translational and rotational vibrations form a bond between oxygen atom from one anion and carbon atom from the other creating intermediate thermodynamically unstable $[OCOCO_2]^{2-}$ anions, each of which decomposes shortly afterward to energetically stable CO_3^{2-} anion and electrically neutral carbon oxide(II) molecule. As we have shown in Figs. 1, 2, and 3 (due to space limitations we did it only for three oxalates, but this is true for all cases) respective oxalate and carbonate structures are very similar (decomposition process of anhydrous alkali metal oxalate is an example of topochemical reaction), thus the process of structure alteration from transitional structure (a result of creating carbonate anion in cationic sub-lattice of anhydrous oxalate) to respective carbonate can undergo relatively easy.

Summing up, the results presented in this paper allow us to state, that despite the fact that our theoretical approach faced some problems related to the process of bond forming during thermal decomposition of anhydrous alkali metal oxalates (C–O bonds), taking into account in our analysis also, apart from direct properties of chemical bond, factors related to the properties of particular atoms, shed some light on the bonding properties and their relation to particular thermal decomposition pathway and allowed us to formulate consistent picture of thermal decomposition of these compounds and to propose the most probable sequence of elementary bond breaking/creating steps taking place during this process, resulting in respective carbonate and carbon oxide(II) as a final products.

Finally, we would like to add one comment of a general nature considering the set of theoretical methods we used in presented analysis. The limitations of quantum mechanical methods applied to periodic solids are well-known and besides them one have to be also aware of the fact that electronic structure calculations within DFT formalism (the same applies to HF method) are done for stationary state which means that we can get the information (quite precise we may add) only for the initial state. The rest is of more or less hypothetical nature, but on a basis of additional data (from BVM analysis) providing us with some information about strains acting on particular bonds, local atomic environments, and overall structural deviation from ideal one, one can infer (even if mostly qualitatively) the most probable behavior of the structure in one or two next steps of thermal decomposition process, namely how the electron charge should flow and bond lengths change, both resulting in strain relaxation and thus bonds strength change, which usually is sufficient to allow one to propose the most probable sequence of consecutive steps leading to a final structure. In case of two step decomposition process this is even more difficult due to the necessity of taking into account the additional processes of bond formation, but even in this case, as we tried to show in this paper, it is possible to get some important insight into the thermal decomposition process and find the highly probable source of its different pathway in comparison with transition metal oxalates. One could try to use alternative approaches to get more quantitative results, e.g., molecular dynamics simulations or separate calculations for all possible consecutive transition states starting from initial structure up to the final one, but first of all this is not possible with the proposed approach based on this particular type of quantum mechanical calculations and it would require a choice of different methods, second it would be very tedious and time and resources consuming process and

third, we are quite convinced that at the end, one would not get considerably more valuable information about thermal decomposition process in oxalates, resulting in an overall picture of thermal decomposition process, which would be significantly different than the one we propose.

Acknowledgments This study was supported by AGH-UST Grant No. 11.11.160.110.

References

1. Koleżyński A, Małecki A. Theoretical studies of electronic structure and structural properties of anhydrous alkali metal oxalates. Part I. electronic structure and electron density topology calculations. J Therm Anal Cal. Accepted. doi:10.1007/s10973-013-3126-z.
2. Małecka B, Drożdż-Cieśla E, Małecki A. Mechanism and kinetics of thermal decomposition of zinc oxalate. Thermochim Acta. 2004;423:13–8.
3. Brown ME, Dollimore D, Galwey AK. Comprehensive chemical kinetics. In: Bamford CH, Tipper CFH, editors. Reactions in solid state vol 2. Amsterdam: Elsevier; 1980.
4. Boldyrev VV, Nevyantsev IS, Mikhailov YI, Khayretdinov EF. K voprosu o myekhanizmye tyermichyeskogo razlozhyeniya oksalatov. Kinet Katal. 1970;11:367–73.
5. Borchardt HJ, Daniels F. The application of differential thermal analysis to the study of reaction kinetics. J Am Chem Soc. 1957;79:41–6.
6. Dollimore D. The thermal decomposition of oxalates. A review. Thermochim Acta. 1987;117:331–63.
7. Randhawa BS, Kaur M. A comparative study on the thermal decomposition of some transition metal maleates and fumarates. J Therm Anal Cal. 2007;89(1):251–5.
8. Galwey AK, Brown ME. An appreciation of the chemical approach of V. V. Boldyrev to the study of the decomposition of solids. J Therm Anal Cal. 2007;90(1):9–22.
9. Fujita J, Nakamoto K, Kobayashi M. Infrared spectra of metallic complexes. III. The infrared spectra of metallic oxalates. J Phys Chem. 1957;61(7):1014–5.
10. Nopsiri Ch, Rangson M, Surasak N, Banjongchom B, Panpailin S, Naratip V. Non-isothermal kinetics of the thermal decomposition of sodium oxalate $Na_2C_2O_4$. J Therm Anal Cal. 2012;107(3):1023–9.
11. Błażejowski J, Zadykowicz B. Computational prediction of the pattern of thermal gravimetry data for the thermal decomposition of calcium oxalate monohydrate. J Therm Anal Cal. 2013. doi:10.1007/s10973-012-2934-x.
12. Bader RFW. Atoms in molecules: a quantum theory. Oxford: Clarendon Press; 1990.
13. Brown ID. The chemical bond in inorganic chemistry. The bond valence model. Oxford: Oxford University Press; 2002.
14. Koleżyński A, Małecki A. Theoretical studies of thermal decomposition of anhydrous cadmium and silver oxalates. Part I. Electronic structure calculations. J Therm Anal Cal. 2009;96(1):161–5.
15. Koleżyński A, Małecki A. Theoretical studies of thermal decomposition of anhydrous cadmium and silver oxalates. Part II. Correlations between the electronic structure and the ways of thermal decomposition. J Therm Anal Cal. 2009;96(1):167–73.
16. Koleżyński A, Małecki A. First principles studies of thermal decomposition of anhydrous zinc oxalate. J Therm Anal Cal. 2009;96(2):645–51.
17. Koleżyński A, Małecki A. Theoretical approach to thermal decomposition process of chosen anhydrous oxalates. J Therm Anal Cal. 2009;97(1):77–83.
18. Koleżyński A, Małecki A. Theoretical analysis of electronic structure and structural properties of anhydrous calcium oxalate. J Therm Anal Cal. 2009;99(2):947–55.
19. Koleżyński A, Małecki A. Theoretical analysis of electronic and structural properties of anhydrous mercury oxalate. J Therm Anal Cal. 2010;101(2):499–504.
20. Koleżyński A, Handke B, Drożdż-Cieśla E. Crystal structure, electronic structure and bonding properties of anhydrous nickel oxalate. J Therm Anal Cal. 2013; (in print). doi:10.1007/s10973-012-2844-y.
21. Pauling L. The principles determining the structure of complex ionic crystals. J Amer Chem Soc. 1929;51:1010–26.
22. Urusov VS, Orlov IP. State-of-art and perspectives of the bond-valence model in inorganic crystal chemistry. Crystallogr Rep. 1999;44:686–709.
23. Brown ID, Shannon RD. Empirical bond-strength-bond-length curves for oxides. Acta Cryst. 1973;A29:266–82.
24. Dollimore D, Tinsley D. The thermal decomposition of oxalates. Part XII. The thermal decomposition of lithium oxalate. J Chem Soc. 1971; A:3043–3047. doi:10.1039/J19710003043.
25. Girgis MM, El-Awad AM. Kinetics and mechanism of thermal decomposition of lithium oxalate catalysed by $Cd_{1-x}Co_xFe_2O_4$($x = 0.0$, 0.5 and 1.0) ferrospinel additives. Thermochim Acta. 1993;214:291–303.
26. Galwey AK, Brown ME. Thermal decomposition of ionic solids. vol. 86: chemical properties and reactivities of ionic crystalline phases (studies in physical and theoretical chemistry).Amsterdam: Elsevier Science; 1999.
27. Effenberger H, Zemann J. Verfeinerung der kristallstruktur des lithiumkarbonates, Li_2CO_3. Z Kristallographie. 1979;150:133–8.
28. Yoshimori T, Asano Y, Toriumi Y, Shiota T. Investigation on the drying and decomposition of sodium oxalate. Talanta. 1978;25:603–5.
29. Ballivet-Tkatchenko D, Galy J, Parize JL, Savariault JM. Thermal decomposition of sodium oxalate in the presence of V 2O 5: mechanistic approach of sodium oxibronzes formation. Thermochim Acta. 1994;232:215–23.
30. Dusek M, Chapuis G, Meyer M, Petricek V. Sodium carbonate revisited. Acta Crystallogr B. 2003;59:337–52.
31. Dinnebier RE, Vensky S, Jansen M, Hanson J. Crystal structures and topological aspects of the high-temperature phases and decomposition products of the Alkali-metal oxalates $M_2[C_2O_4]$ (M=K, Rb, Cs). Chem Eur J. 2005;11:1119–29.
32. Masuda Y, Ito R, Matsuda T, Ito Y. The thermal phase transition of anhydrous potassium oxalate. Thermochim Acta. 1988;131:291–6.
33. Papazian HA, Pizzolato PJ, Patrick JA. Thermal decomposition of oxalates of ammonium and potassium. J Am Cer Soc. 1971;54:250–4.
34. Kahwa IA, Mulokozi AM. The thermal decomposition temperatures of ionic metal oxalates. J Therm Anal. 1981;22:61–5.
35. Ito R, Masuda Y, Ito Y. Thermal analyses of rubidium and cesium oxalate monohydrates. Thermochim Acta. 1988;127:159–70.